ELSEVIER

Journal of Fluids and Structures 19 (2004) 111–122

JOURNAL OF FLUIDS AND STRUCTURES

www.elsevier.nl/locate/jnlabr/yjfls

Active control of flow oscillations in jet–wedge system by acoustic feedback

N. Fujisawa*, Y. Takizawa, T. Kohno, S. Tomimatsu

Department of Mechanical and Production Engineering, Niigata University, 8050 Ikarashi 2, Niigata 950-2181, Japan

Received 18 March 2002; accepted 26 September 2003

Abstract

The performance and mechanism of an acoustic feedback control applied to flow oscillation in a jet–wedge system were investigated experimentally. The self-sustained oscillations were effectively suppressed by imposing velocity fluctuations near the nozzle exit, which were fed by the fluctuating pressure signal at the wedge with a certain phase lag and feedback gain. The optimum condition for the imposed velocity amplitude was found to be as small as 1.2% of the jet velocity. The variation of the flow field with and without control was studied by flow visualization with high-speed camera and by flow-field measurements with particle image velocimetry. These observations indicate that the primary mode of the jet oscillation in the jet–wedge system is weakened by the feedback control to a level of secondary mode. This is mainly due to the destruction of the synchronized flow structure of the jet–wedge system by the active control, which is found in the mean and fluctuating velocity distribution and the velocity correlation over the wedge and along the jet shear-layers.

1. Introduction

The impingement of a planar jet on a wedge produces a sound of discrete frequency, which is called edge tone. The mechanism of edge-tone generation has been studied by many researchers in literature, which are summarized in some review papers by Rockwell and Naudasher (1979), Blake and Powell (1984), and others. It is known that the generation of the edge-tone is due to the self-sustained feedback mechanism created by the interaction of the jet with the wedge. This interaction process is followed by the feedback of the fluctuating pressure to the upstream causing the amplified shear-layer instability at the most receptive region near the nozzle exit, which results in vorticity amplification of the jet flow. It should be mentioned that the jet–wedge interaction causes pressure fluctuations on the lower and upper surfaces of the wedge, which are opposite in phase with respect to each other. This is due to the presence of a dipole-like source at the leading edge of the wedge (Powell, 1961; Staubli and Rockwell, 1987). Details of the unsteady nature of the flow on the jet–wedge system are described by Kaykayoglu and Rockwell (1986a, b) and the PIV measurements of the flow field around the wedge are reported by Lin and Rockwell (2001).

Recently, the feedback control of unstable flow phenomenon has received considerable attention from the point of view of a fundamental interest as well as practical applications. The feedback control was applied to the fundamental flows, such as the vortex shedding from a circular cylinder (Ffowcs Williams and Zhao, 1989; Roussopoulos, 1993; Warui and Fujisawa, 1996; Fujisawa et al., 2001), the flow over cavities (Huang and Weaver, 1991; Kikuchi and Fukunishi, 1999) and the separating shear layers (Kiya et al., 1999). It is also applied to the practical problems, which covers the flow control in the fluid machinery (Ffowcs Williams and Huang, 1989; Huang and Weaver, 1994) and the

*Corresponding author. Tel./fax: +81-25-262-6726.
E-mail address: fujisawa@eng.niigata-u.ac.jp (N. Fujisawa).

0889-9746/$ - see front matter
doi:10.1016/j.jfluidstructs.2003.09.001

combustion oscillations (Langhorme et al., 1990), and so on. These studies indicate that the feedback control is very effective for controlling the unsteady flow phenomena in engineering problems.

On the contrary, the feedback control was applied to the jet–wedge system by Ziada (1995), who used the microphone as the feedback sensor and the loud speakers for controlling the edge tone generated from the jet–wedge system. It was demonstrated that the feedback control is very effective in reducing the edge tone generated by the wedge, which is also supported by the qualitative visualization pictures produced by a smoke injection technique. Later, this problem was treated in the preliminary report of the present study to understand the effect of control parameters on the performance of flow control (Fujisawa et al., 2000). However, the modification of the flow field and the control mechanism by the feedback control are still not clear. It should be mentioned that there is very little information on the flow around the wedge under the control.

The purpose of the present paper is to study the optimum performance of the feedback control quantitatively and discuss the mechanism of flow control by visualizing the flow with high-speed camera and measuring the flow properties by PIV with and without control.

2. Experimental apparatus and procedures

2.1. Experimental apparatus

The present experiment was carried out using an open-jet type wind tunnel. The schematic diagram of the test-section is shown in Fig. 1. The exit dimensions of the contraction nozzle are 20 mm in height and 200 mm in width. The wedge has a sharp angle of 28° and is situated downstream of the contraction nozzle. It is followed by a flat plate in the downstream having a cross-section of 20 mm × 200 mm and is 400 mm long. The plate was supported by the vertical sidewalls, which were 200 mm in height and 600 mm in length. The wedge and the sidewalls are made of transparent material for flow visualization purposes. The distance between the wedge apex and the nozzle exit can be varied by traversing the wedge along the grooves over the sidewalls. The details of the wedge structure are shown in a blow up in Fig. 1. Two pressure holes of 1 mm in diameter were drilled over the wedge surfaces, which are located at the middle of the wedge surface at a distance of 22 mm from the apex. The surface pressures were detected by pressure transducers of strain-gauge type. The pressure hole and the transducer are connected by a stainless-steel pipe having an inner diameter of 2 mm. The frequency response of the measurement system including the piping was found to be flat up to 150 Hz.

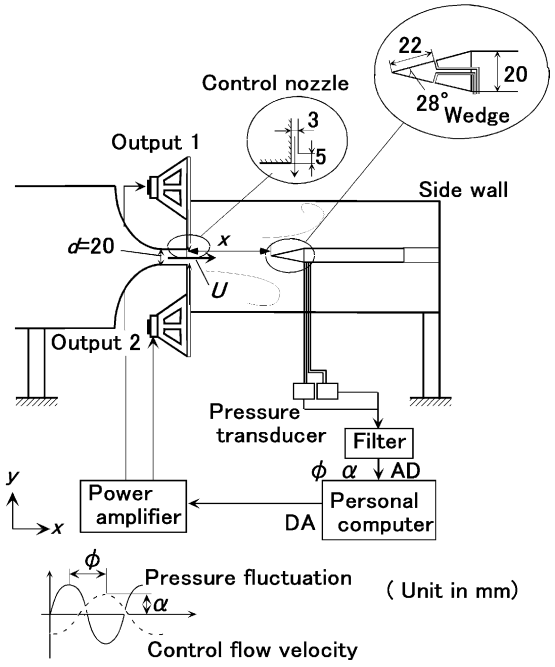

Fig. 1. Experimental test-section for feedback control of jet–wedge system.

The pressure fluctuations on the wedge surface are measured at the nozzle exit velocities of 10, 15 and 20 m/s, which correspond to the Reynolds numbers ($Re = Ud/v$) of 1.3×10^4, 2.0×10^4, 2.7×10^4, respectively, where v is a kinematic viscosity of the fluid. The flow visualization and the PIV measurement of the instantaneous velocity-field were carried out at $Re = 2.0 \times 10^4$. It is noted that the streamwise turbulence intensity at the nozzle exit was about 1% of the jet velocity. The measured frequency spectrum does not indicate any noticeable peak in the present experiment.

2.2. Feedback control

The pressure signal detected over the wedge surface was used as a feedback signal in the present experiment. The signal was fed back to the speaker system located near the nozzle exit through the AD and DA converter. The phase and the gain of the signal were set in digital form by a personal computer and the output signal was power-amplified by a DC amplifier to meet with the power level of the speaker system. Details of feedback control have been described by Fujisawa et al. (2001). The maximum power level of the speaker is 300 W. The details of the speaker system are also displayed in Fig. 1. The height of the speaker nozzle was 3 mm, the width was 200 mm and has an offset height of 5 mm from the nozzle plane. The preliminary experiment suggests that the velocity signal at the exit of the speaker system was delayed by 5–10 ms from the reference pressure signal detected over the wedge surface. This delay can be caused by the effects of viscosity and compressibility of the fluid between the speaker and the nozzle exit. Therefore, the time lag was corrected based on the measurement of phase lag between the pressure signal and the exit velocity at various frequencies in the present experiment. It is noted that the measurement of periodic velocity at the exit of speaker nozzle was carried out using hot-wire anemometry calibrated against the PIV measurements. The latter technique will be described in detail in the next section. The maximum amplitude of the control flow from the speaker nozzle was evaluated from the maximum velocity and was nondimensionalized by the jet velocity at the nozzle exit to determine the oscillation amplitude of the control flow α ($= v/U$). It is noted that the spectrum of the sound field generated by the speaker has a high peak at the fundamental frequency of excitation, which is much larger than the peaks at the sub- and super-harmonics of the excitation frequency.

2.3. Flow visualization and PIV measurement

The flow field around an edge was visualized by the smoke injection technique and the flow observation was made at the center plane of the wedge to understand the control mechanism of flow oscillations in the jet–wedge system. The required illumination was given by a laser-sheet from Ar laser of 3 W and the light-sheet plane was observed by a

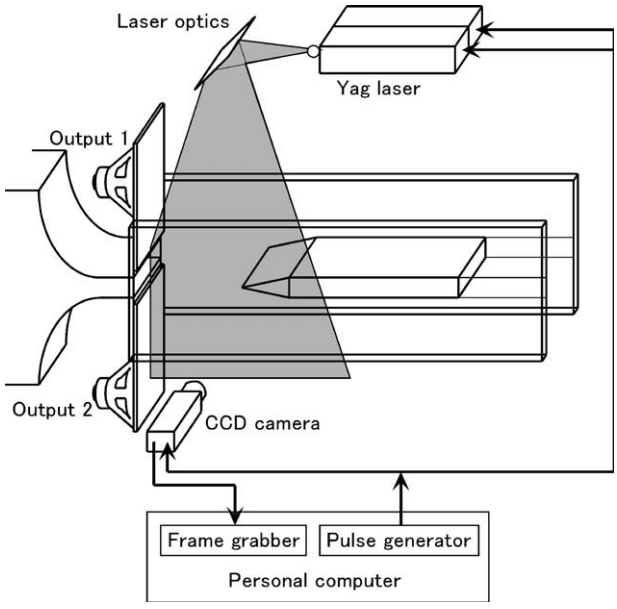

Fig. 2. Experimental arrangement for PIV measurement.

high-speed CCD camera having a maximum frame rate of 2000 frame/s with a spatial resolution of 256×240 pixels. The simultaneous sampling of the pressure signal at the wedge was carried out using an AD converter at the same instant of flow observations. For details of simultaneous visualization and the data sampling see Warui and Fujisawa (1996).

The quantitative measurement of the flow field was carried out using particle image velocimetry. A schematic illustration of the measuring system is shown in Fig. 2. Smoke particles generated from the smoke machine were used as the tracers for measurement. The lasers used in the present PIV measurement are a pair of Nd: YAG lasers, which emit 532 nm wavelength light at a pulse repetition rate of 15 Hz. The highest pulse energy of these lasers is 50 mJ per pulse, which was strong enough to observe the smoke particles by the monochrome digital CCD camera having a spatial resolution of 1018×1008 pixels with 8 bits in gray level. The camera was operated in a double exposure mode and synchronized with the pulse signal from a pulse generator connected to the personal computer, which also controls the triggering of the laser illumination. The time interval between the laser pulses is set to 40 μs in the present measurement. The captured digital images were stored on a frame memory in a personal computer. The target image in the present experiment has actual sizes of 100 mm × 100 mm, so that the spatial resolution is 0.1 mm/pixel. The instantaneous velocity distributions are obtained by using an algorithm based on gray level difference method for the cross-correlation calculation between the two successive images. The sizes of interrogation window and search window were set to 34×34 pixels and 41×41 pixels, respectively, which combination was found to minimize the error vectors with sufficient spatial resolution. The sub-pixel interpolation process was incorporated into this analysis to improve the accuracy of velocity measurement. The statistical properties of the flow field were obtained by averaging over 300 instantaneous velocity distributions.

3. Results and discussions

3.1. Basic characteristics of jet–wedge system

The flow characteristics of the present jet–wedge system are studied by measuring the fluctuating pressure coefficient $C_{p'}$ $(= 2\sqrt{\overline{p'^2}}/\rho U^2)$ over the wedge surface and the Strouhal frequency $\mathrm{St}(= fd/U)$ of flow oscillations (d is the nozzle height, f the frequency, U the free-stream velocity, p' the fluctuating pressure, ρ the density of fluid). Fig. 3 shows the variations of these properties with respect to the distance x/d of the wedge apex measured from the nozzle exit. It is clearly seen that the fluctuating pressure becomes a maximum at $x/d = 5$, where the jet–wedge interaction becomes very strong due to the feedback mechanism of the pressure fluctuations created over the wedge surface. This peak value of the fluctuating pressure is slightly enhanced by increasing the Reynolds number in the present experiment. On the contrary, the Strouhal frequency decreases gradually with an increase in the wedge distance x/d without any noticeable Reynolds number effect. These fundamental properties reported here agree qualitatively with the experiments in a literature (Rockwell and Naudasher, 1979). It is to be noted that the measurement uncertainty of $C_{p'}$ and St are estimated to be 5.2% and 5.0%, respectively, with uncertainty interval of 95% coverage.

3.2. Effect of feedback control

Fig. 4 shows the variation of the fluctuating pressure coefficient $C_{p'}$ on the wedge surface with respect to the phase lag ϕ in the feedback control, where the feedback gain was set to a constant value. The wedge was fixed at a distance $x/d = 5$ and the Reynolds number was kept at $\mathrm{Re} = 2.0 \times 10^4$. The two speakers were operated in opposite phases to maximize the control effect (Fujisawa et al., 2000). It is expected that the perturbed flow comes out from the one of the speaker nozzle and goes into the other speaker nozzle, when they are operated in opposite phase without the jet flow. The fluctuating pressure coefficient $C_{p'}$ is found to vary with the phase lag ϕ between the pressure signal at the wedge and the velocity signal of the control flow. The distribution of $C_{p'}$ shows a local minimum at a phase lag of $\phi = 280^\circ$, which is followed by that of $\phi = 640^\circ$. The phase difference between the first and the second local minimum is 360°, which indicates a close agreement of the oscillating frequency of the jet flow with control to that without control, because the phase is estimated with reference to the frequency without control. The reason why the phase lag at the local minimum of $C_{p'}$ does not meet with the opposite phase condition, that is $\phi = 180^\circ$, is expected to be due to the distance the disturbance has to travel from the exit of the control nozzle to the detecting position of pressure at the wedge, where the opposite phase conditions meet. The slight increase in $C_{p'}$ at the second local minimum in comparison with the first one can be caused by the reduced correlation between the pressure and the flow field around the wedge. It is noted that the minimum $C_{p'}$ is smaller than that without control. Therefore, the oscillations in the jet–wedge system are weakened, when the phase lag is set to an optimum value. In order to examine the influence of the velocity

magnitude from the slit, the amplitude of control flow α ($= v/U$) was evaluated at the local minimum of $C_{p'}$ and was found to be $\alpha = 0.012$. This condition suggests that the jet–wedge interaction can be optimally controlled by imposing a small control flow having a magnitude of only 1.2% of the jet velocity.

Fig. 5 gives the variation of fluctuating pressure coefficient $C_{p'}$ over the wedge surface with respect to the amplitude of control flow α, where the phase lag ϕ was set to an optimum phase 280°. The fluctuating pressure coefficient $C_{p'}$ decreases suddenly with an increase in α and reaches a minimum at $\alpha = 0.012$, while it increases gradually with further increases in α. It is to be noted that $C_{p'}$ at $\alpha = 0$ corresponds to the fluctuating pressure coefficient without feedback control. These results indicate the presence of optimum value α for reducing the fluctuating pressure. Similar results have been obtained in the experiments by Roussopoulos (1993) and Fujisawa et al. (2001) and by a stability analysis by Monkewitz (1989), who suggested that the increase in $C_{p'}$ with α is likely due to the instability at a different mode.

The optimum combinations of the phase lag ϕ and the amplitude of control flow α at various positions of the wedge from the nozzle were obtained by trial and error in the present experiment. The results are shown in Fig. 6, where the optimum phase lag ϕ_0 and the amplitude of control flow α_0 are plotted against the wedge distance x/d. The Reynolds number of the present experiment is $\mathrm{Re} = 2.0 \times 10^4$. The optimum phase lag seems to be constant for all the wedge distances x/d considered. This result suggests that the mode of the jet oscillation under the optimum control does not change with wedge distance. On the contrary, the optimum amplitude of the control flow α_0 does change with wedge distance. The distribution of α_0 may be influenced by the variation of $C_{p'}$ at the wedge with the wedge distance.

Fig. 7 shows the variations of the fluctuating pressure coefficient $C_{p'}$ with respect to the wedge distance x/d under the optimum feedback control, in comparison with those without control. The present result indicates that the fluctuating pressure coefficient $C_{p'}$ under the control is decreased for every x/d in comparison with the case without control. The reduction in $C_{p'}$ is very large around the peak of $C_{p'}$, that is, $x/d = 5-8$. It should be mentioned here that the

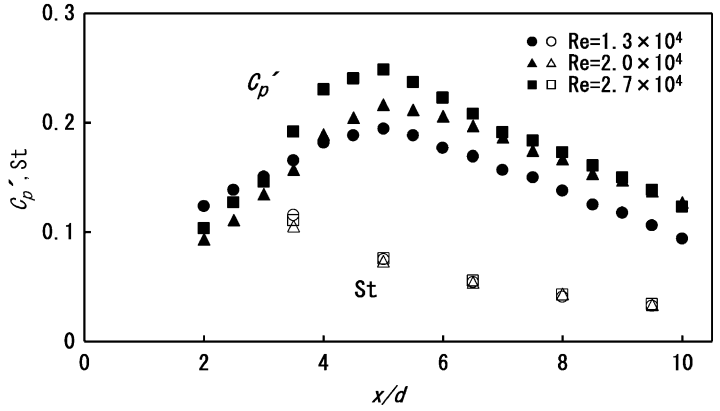

Fig. 3. Distributions of fluctuating pressure coefficient $C_{p'}$ and Strouhal number St in jet–wedge system.

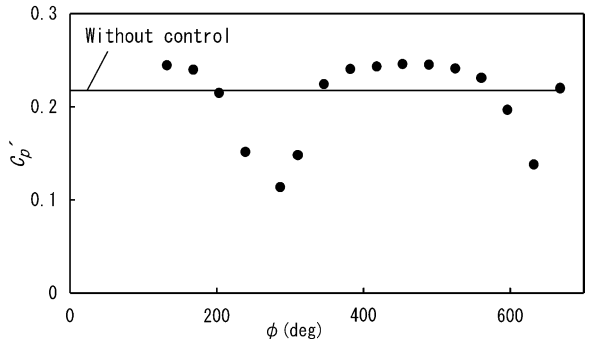

Fig. 4. Effect of phase lag ϕ at optimum amplitude of control flow ($x/d = 5$, $\mathrm{Re} = 2.0 \times 10^4$).

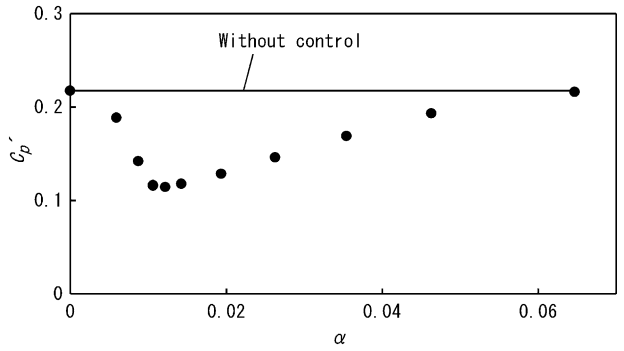

Fig. 5. Effect of velocity amplitude α on fluctuating pressure coefficient $C_{p'}$ at optimum phase lag ($x/d = 5$, $\mathrm{Re} = 2.0 \times 10^4$).

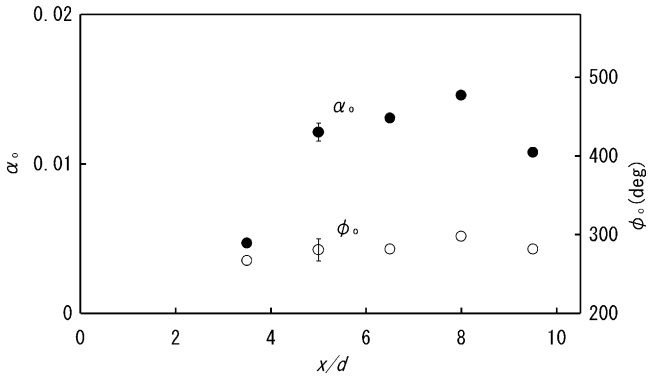

Fig. 6. Distributions of optimum control parameters ϕ_0 and α_0 ($\mathrm{Re} = 2.0 \times 10^4$).

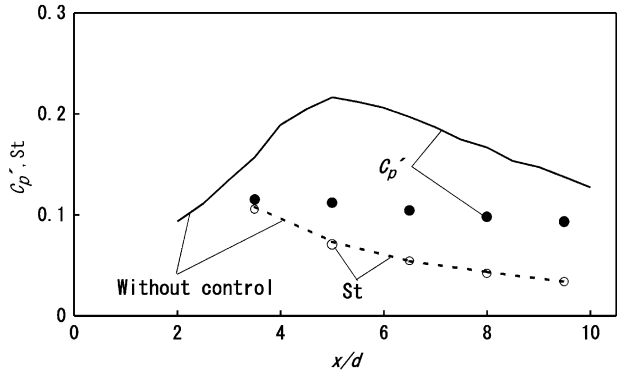

Fig. 7. Distributions of fluctuating pressure coefficient $C_{p'}$ and Strouhal number St under optimum feedback control ($\mathrm{Re} = 2.0 \times 10^4$).

fluctuating pressure coefficient of the plane free jet is found to be 0.08 in the present experiment, which is measured by a static-pressure tube in the present study. Therefore, the fluctuating pressure coefficient under the optimum feedback control is close to that for the plane free jet. On the contrary, the Strouhal frequency St under the optimum control varies in the same manner as that without feedback control in the range of parameters for present study, which indicates that the mode of the jet oscillation is not greatly influenced by the feedback control.

3.3. Flow visualization

Simultaneous visualization of the flow with respect to the pressure signal at the wedge was carried out using a high-speed CCD camera to examine the effect of feedback control on the flow field. The flow visualization study was conducted at $\mathrm{Re} = 2.0 \times 10^4$ and the wedge distance was set at $x/d = 5$, where the maximum amplification of pressure fluctuations is observed in the present experiment as shown in Fig. 3. Typical visualization images over the wedge surface without the control are shown in Fig. 8, where sequential 6 images are displayed at time intervals of 3 ms. The corresponding pressures at the wedge are plotted against time in the pressure chart shown below the visualization pictures. The visualized flow field (a) indicates that the jet flow is switching from the upper surface to the lower surface of the wedge, which results in an asymmetrical smoke formation on both surfaces. Therefore, the smoke on the upper surface is distributed over a much wider area over the edge than that on the lower surface. It is expected from the flow pattern that the velocity on the upper surface is higher than that on the lower surface, which corresponds to a lower pressure on the upper surface and the higher pressure on the lower surface. This conclusion is further substantiated by the measured pressure fluctuation at the wedge, which indicates that the lowest pressure is created on the upper surface. With an advance in frame image (b), the deflection of the jet flow reaches the maximum on the lower surface of the wedge. Therefore, the velocity is decreased on the upper surface and increased on the lower surface in comparison with the picture (a), so that the pressure at the wedge is increased as shown in the pressure traces. The flow images (c) and (d) show the deflection of the jet flow to the upper surface, which is followed by the jet deflection to the lower surface (e) and (f). It can be concluded that the flow pattern in front of the wedge is fairly periodic in nature and the variation of the flow pattern matches well with the variation of pressure traces measured at the wedge. It is to be noted that the formation of the smoke pattern over the wedge is delayed due to the deflection of the jet flow in front of the wedge,

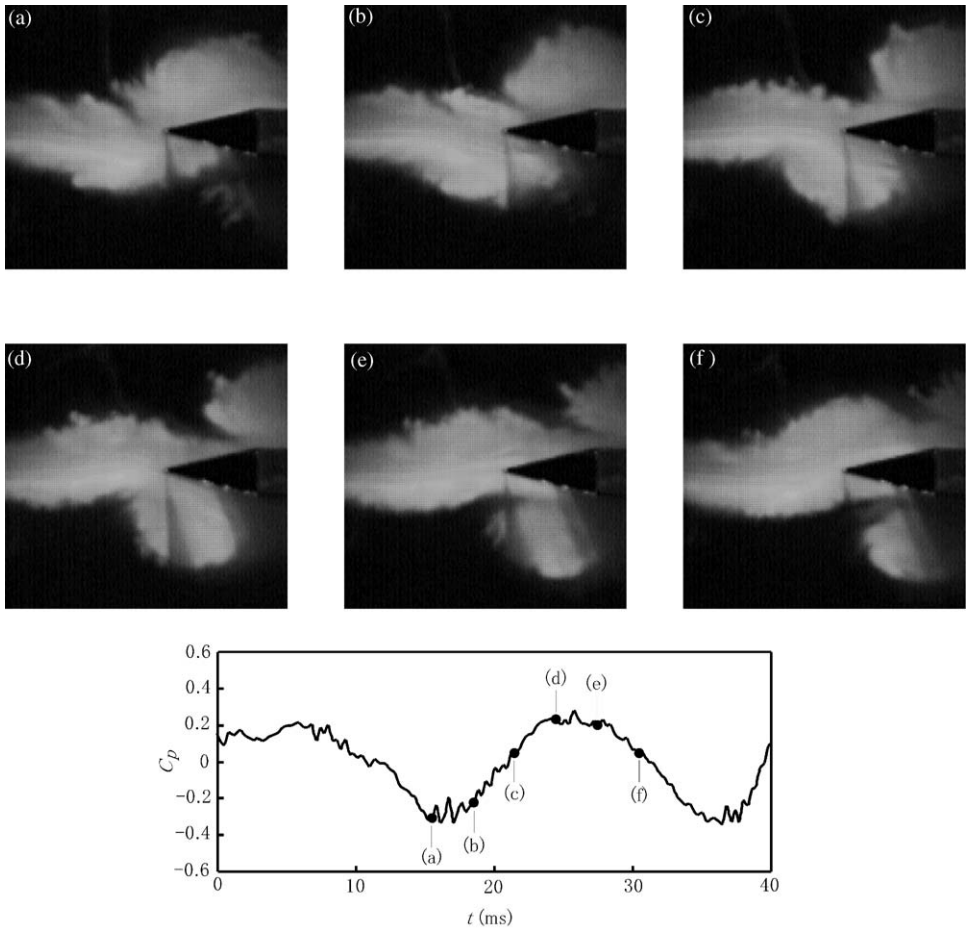

Fig. 8. Simultaneous flow visualization and pressure fluctuation at the wedge without control ($x/d = 5$, $\mathrm{Re} = 2.0 \times 10^4$).

which reflects the unsteady effect of the jet flow around the wedge. Therefore, it is very difficult to understand the flow physics from such a qualitative visualization of the unsteady flow, which suggests an importance of flow measurements by PIV presented in the following section.

Typical flow visualization results around the wedge under the optimum feedback control are shown in Fig. 9. These pictures are selected at every 3 ms intervals to compare with the flow visualization pictures without control shown in Fig. 8. The corresponding pressure chart is shown below the pictures, which indicates very strong suppression of pressure oscillation by the control. Further, the oscillating frequency of pressure is modulated by the presence of both the primary frequency and the double frequency, which was also confirmed by the spectrum analysis of the pressure fluctuations (Fujisawa et al., 2000). It is found from the visualization pictures that the oscillation of the jet flow, as observed in the flow visualization pictures without control, is almost diminished in the visualization pictures under the optimum control. Therefore, the instantaneous flow field around the wedge is very similar to each other independent of time, which suggests the strong suppression of primary mode of the jet oscillation. On the other hand, the observation of the smoke in front of the wedge shows the presence of secondary mode of jet oscillation at double frequency of the primary mode. Therefore, the jet oscillation in the secondary mode was not suppressed by the introduction of acoustic feedback at the primary mode. There might be some contributions to the secondary mode from the harmonics of the excitation frequency of the speaker itself.

3.4. Measurement of statistical properties of flow around the wedge

In order to understand the flow field under the acoustic feedback quantitatively, the measurement of statistical properties of the flow field is carried out using the particle image velocimetry at the same experimental condition as the

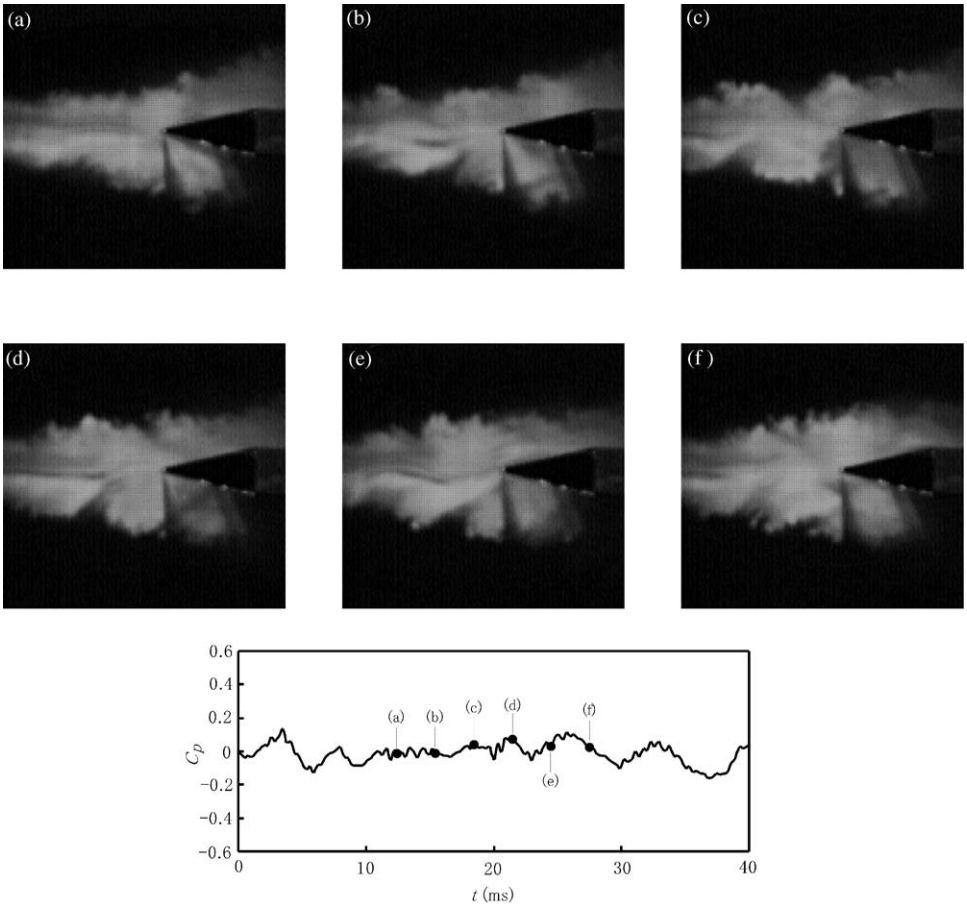

Fig. 9. Simultaneous flow visualization and pressure fluctuation at the wedge under optimum feedback control ($x/d = 5$, $\mathrm{Re} = 2.0 \times 10^4$).

flow visualization. Fig. 10(a) shows the distribution of the time-averaged velocity magnitude around the wedge without control. The potential core region, where the flow keeps the velocity at the nozzle exit, is formed downstream of the nozzle and it prevails up to $x/d = 4$. This region is separated into two shear layers as the flow approaches the wedge. The deceleration of the flow is obvious in front of the wedge, which indicates the influence of flow oscillations in the jet–wedge system. It is to be noted that these features of the flow field without control agree with the measurements by Lin and Rockwell (2001). On the contrary, the distribution of the velocity magnitude is modified by the optimum feedback control, as shown in Fig. 10(b). The potential core region is elongated to the downstream and it prevails up to $x/d = 4.5$ under the feedback control. The comparative study of the flow over the wedge with and without feedback control indicates that the velocity magnitude is increased over the wedge surface and the flow is concentrated to the near-wedge-region under the feedback control, which suggests the suppression of the flow oscillations by the feedback control. It is

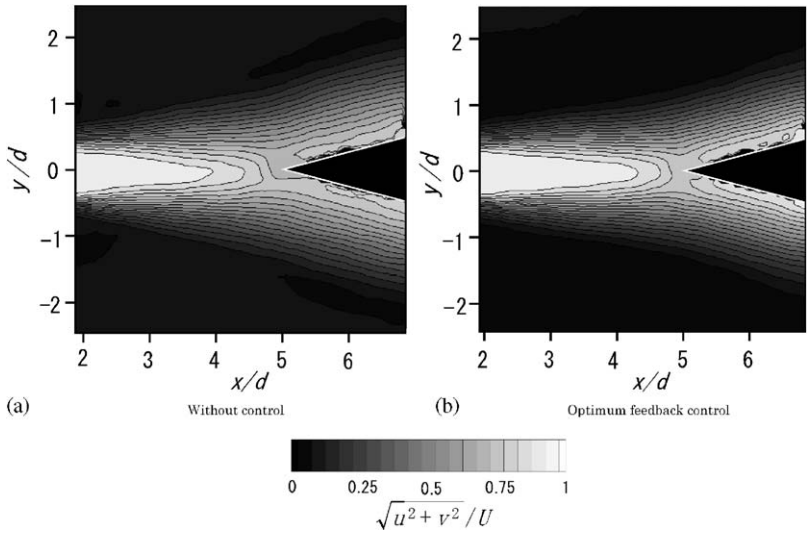

Fig. 10. Distributions of velocity magnitude around wedge ($x/d = 5$, $\mathrm{Re} = 2.0 \times 10^4$): (a) without control and (b) optimum feedback control.

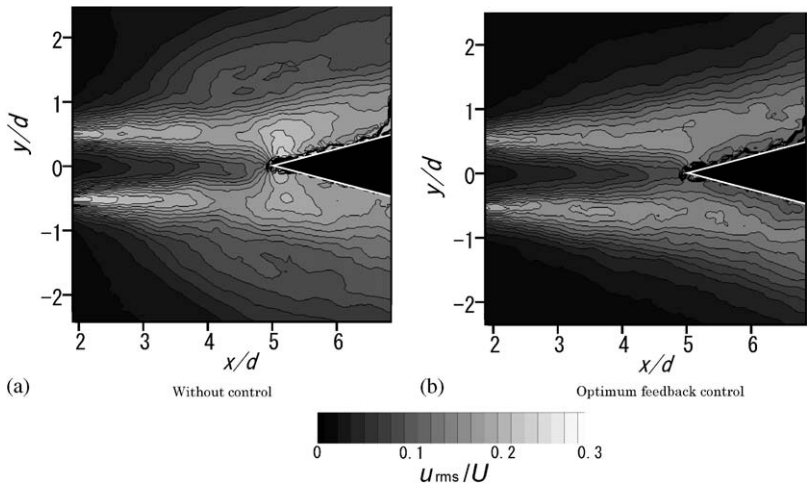

Fig. 11. Distributions of streamwise velocity fluctuation $u_{\mathrm{r.m.s.}}/U$ around wedge ($x/d = 5$, $\mathrm{Re} = 2.0 \times 10^4$): (a) without control and (b) optimum feedback control.

to be noted that a noisy structure appears very close to the wedge surface, which is due to the appearance of unexpected erroneous vectors near the oblique wall in the PIV analysis.

Fig. 11(a) shows the distribution of streamwise component of velocity fluctuations $u_{\mathrm{r.m.s.}}/U$ around the wedge without control. It is clear that the streamwise velocity fluctuations become large along the two shear layers between the nozzle and the wedge, which is expected to be due to the self-sustained flow oscillations of the jet–wedge system. A region of large velocity fluctuations is also formed in a direction normal to the jet flow near the wedge apex. The velocity fluctuations along the jet flow are created on both sides of the jet potential core, where the velocity gradient becomes large. They are further enhanced by the flow oscillations created near the wedge apex. This result supports the explained mechanism of self-sustained flow oscillations in the jet–wedge system. When the feedback control is applied to the jet–wedge system, the velocity fluctuations are weakened in the whole flow field. A significant reduction was observed especially in the velocity fluctuations near the wedge apex. These results indicate that the feedback control is very effective in suppressing the flow oscillations created at the wedge by the acoustic excitation imposed on the jet shear-layer near the nozzle exit.

Figs. 12(a) and (b) show the distribution of the velocity fluctuations normal to the jet axis $v_{\mathrm{r.m.s.}}/U$ without and with control, respectively. Under the self-sustained flow condition in Fig. 12(a), the normal velocity fluctuations are considerably enhanced along the shear layers and near the wedge apex, which is similar to the observation of streamwise velocity fluctuations in Fig. 11(a). However, a region of large velocity fluctuations is created in front of the wedge, which is due to the predominant motion of flow oscillations normal to the jet axis in front of the wedge. This region prevails to the side of the wedge and forms the region of large velocity fluctuations in the jet shear layer from the nozzle. It is to be noted that the region of large normal velocity fluctuations is shifted to the outside of the wedge in comparison with that of the streamwise velocity fluctuations. This result suggests that the influence of flow oscillation is more widely observed in the normal velocity fluctuations. On the contrary, the smaller velocity fluctuations prevail over the wedge surface due to the constraint condition at the wedge to suppress the velocity fluctuations normal to the surface. On the other hand, the velocity fluctuations near the wedge apex are fairly reduced by the feedback control, and the area over which the normal velocity fluctuations around the wedge is decreased in comparison with the case without control, as was observed in the streamwise velocity fluctuations.

Figs. 13(a) and (b) show the distribution of Reynolds shear-stress $\overline{uv}/U^2$ around the wedge without and with feedback control, respectively. Again, the influence of jet oscillation is felt very clearly near the wedge apex in Fig. 13(a) and the region of large magnitude of shear stress prevails over the wedge and along the jet shear layers developing from the nozzle. It should be noted that the opposite sign of the shear stress results from the shear layer near the wedge apex, which indicates the overshoot of the shear stress distribution. On the other hand, the increase in shear stress magnitude is effectively suppressed by the feedback control in Fig. 13(b) and the width of the dominant region of shear stress over the wedge is reduced, which is very similar to the flow field variation by feedback control as observed in Figs. 10–12.

Figs. 14(a) and (b) give the distribution of cross-correlation between the normal velocities without and with control, respectively, where the reference point is fixed in front of the wedge apex. The results without control indicate that the positive correlation is observed along the jet shear-layer prevailing from the wedge apex, which suggests the synchronization of the jet oscillation near the wedge apex with the velocity fluctuation downstream of the wedge. On the contrary, there is a large negative correlation between the flow near the wedge apex and that on both sides of the jet and on the jet centerline, which indicates the presence of synchronized flow structure upstream of the wedge. This result suggests the presence of oscillations of the jet in the opposite direction near the wedge apex $x/d = 5$ and at these upstream locations. Therefore, the flow field around the wedge is well organized and synchronized in structure by the velocity fluctuations normal to the jet flow. It should be mentioned that the synchronization of the flow structure is also observed in the distribution of cross-correlation between the streamwise velocity fluctuations, but the spatial variations in the magnitude of correlation is smaller than that of the normal velocity fluctuations, which suggests an importance of normal velocity fluctuations in the behavior of jet oscillation.

The distribution of correlation between the normal velocity fluctuations is modified by the application of optimum control, which is shown in Fig. 14(b). Although the qualitative nature of the correlation under the control is similar to that without control, the magnitude of the correlation is substantially reduced by the control. This result suggests that the synchronized structure of the jet–wedge system is weakened by the control. It is interesting to note that the position of negative correlation in the jet centerline is shifted to downstream under control conditions, which may correspond to the generation of secondary mode in the jet oscillation observed in the flow visualization study.

These observations of the flow field around the wedge indicate that the flow oscillations in the jet–wedge system are effectively suppressed by the introduction of small velocity fluctuations with feedback control. It is understood that the dipole-like source at the leading-edge of the wedge is weakened by the control, which modifies the upstream influence by weakening the globally synchronized structure of the jet–wedge system.

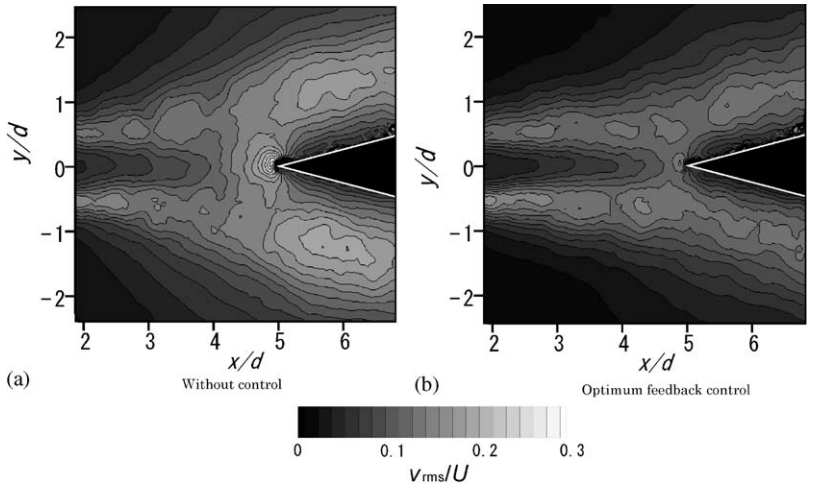

Fig. 12. Distributions of normal velocity fluctuation $v_{\mathrm{r.m.s.}}/U$ around wedge ($x/d = 5$, $\mathrm{Re} = 2.0 \times 10^4$): (a) without control and (b) optimum feedback control.

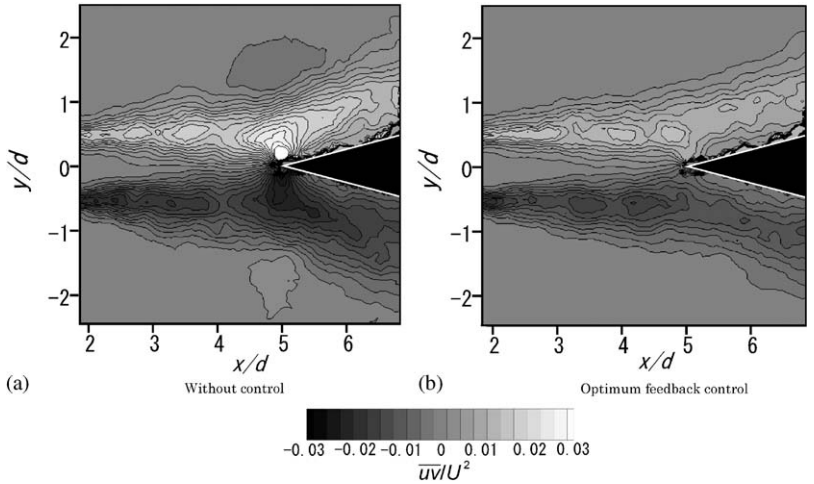

Fig. 13. Distributions of Reynolds shear stress $\overline{uv}/U^2$ around wedge ($x/d = 5$, $\mathrm{Re} = 2.0 \times 10^4$): (a) without control and (b) optimum feedback control.

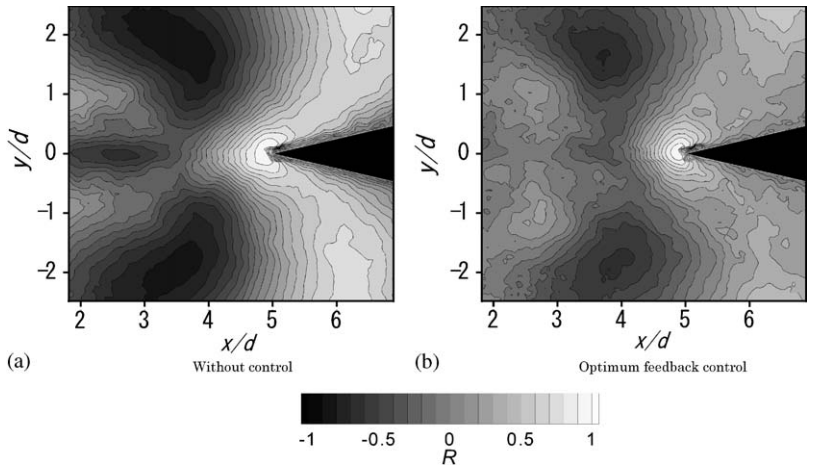

Fig. 14. Distribution of cross-correlation between normal velocity fluctuations: (a) without control and (b) optimum feedback control.

4. Conclusions

The performance and mechanism of an acoustic feedback control applied to flow oscillation in a jet–wedge system were investigated experimentally. The self-sustained flow oscillations were effectively reduced by the control, where the pressure fluctuations at the wedge were fed back to the velocity fluctuations near the nozzle exit. The optimum condition for the imposed velocity amplitude is found to be as small as 1.2% of the jet velocity. The modification of the flow field by the control was studied by the flow visualization and PIV measurements. It was found that the flow oscillation at the primary mode of jet oscillation was substantially weakened by the control to a level of secondary mode having a double frequency. The flow field was modified by the control, especially in front of the wedge and that along the jet shear-layers, where the velocity fluctuations and velocity correlation normal to the jet flow are greatly enhanced by the synchronization of the flow in the jet–wedge system. Therefore, the feedback control acts on the jet shear layer so as to cancel the fundamental mode of the jet–wedge interaction and results in the destruction of the synchronized structure of the flow around the wedge.

Acknowledgements

The authors would like to thank to Dr K. Srinivas of Sydney University for helpful suggestions and Mr N. Ike of the student in Niigata University for his help in the experiment.

References

Blake, W.K., Powell, A., 1984. The development of contemporary views of flow-tone generation. In: Krothapalli, A., Smith, C.A. (Eds.), Recent Advances in Aeroacoustics. Springer, New York, pp. 247–325.

Ffowcs Williams, J.E., Huang, 1989. Active stabilization of compressor surge. Journal of Fluid Mechanics 204, 245–262.

Ffowcs Williams, J.E., Zhao, B.C., 1989. The active control of vortex shedding. Journal of Fluids and Structures 3, 115–122.

Fujisawa, N., Kouno, T., Takano, T., 2000. Basic study on active control of edge tone and control mechanism. Transactions JSME 66, 153–158 (in Japanese).

Fujisawa, N., Kawaji, Y., Ikemoto, K., 2001. Feedback control of vortex shedding from a circular cylinder by rotational oscillations. Journal of Fluids and Structures 15, 23–37.

Huang, X.Y., Weaver, D.S., 1991. On the active control of shear layer oscillations across a cavity in the presence of pipeline acoustic resonance. Journal of Fluids and Structures 5, 207–219.

Huang, X.Y., Weaver, D.S., 1994. Control of flow induced fin vibration by anti-sound. Journal of Sound and Vibration 169, 428–432.

Kaykayoglu, R., Rockwell, D., 1986a. Unstable jet–edge interaction: Part 1 instantaneous pressure fields at a single frequency. Journal of Fluid Mechanics 169, 125–149.

Kaykayoglu, R., Rockwell, D., 1986b. Unstable jet–edge interaction: Part 2 multiple frequency pressure fields. Journal of Fluid Mechanics 169, 151–172.

Kikuchi, S., Fukunishi, Y., 1999. Active flow control technique using piezo-film actuators applied to the sound generation by a cavity. Proceedings of the ASME/JSME Fluids Engineering Conference, FEDSM'99-No. 7232, San Francisco.

Kiya, M., Mochizuki, O., Kudo, D., 1999. Active control of turbulent separated flows. Proceedings of the ASME/JSME Fluids Engineering Conference, San Francisco, FEDSM'99-No. 6956.

Langhorme, P.J., Dowling, A.P., Hooper, N., 1990. Practical active control system for combustion oscillations. Journal of Propulsion and Power 26, 324–333.

Lin, J.-C., Rockwell, D., 2001. Oscillations of a turbulent jet incident upon an edge. Journal of Fluids and Structures 15, 791–829.

Monkewitz, A., 1989. Feedback control of global oscillations in fluid systems. AIAA Paper 89-0991.

Powell, A., 1961. On the edgetone. Journal of the Acoustical Society of America 33, 395–409.

Roussopoulos, K., 1993. Feedback control of vortex shedding at low Reynolds numbers. Journal of Fluid Mechanics 24, 267–296.

Rockwell, D., Naudasher, E., 1979. Self-sustaining oscillations of impinging free shear layers. Annual Review of Fluid Mechanics 11, 67–94.

Staubli, T., Rockwell, D., 1987. Interaction of an unstable planar jet with an oscillating leading edge. Journal of Fluid Mechanics 176, 135–167.

Warui, H.M., Fujisawa, N., 1996. Feedback control of vortex shedding from a circular cylinder by cross-flow oscillations. Experiments in Fluids 21, 49–56.

Ziada, S., 1995. Feedback control of globally unstable flows: impinging shear flows. Journal of Fluids and Structures 9, 907–923.